Proceedings of ASME Turbo Expo 2003
Power for Land, Sea, and Air
June 16-19, 2003, Atlanta, Georgia, USA

GT2003-38209

NEW AIRFOIL DESIGN TO EXTEND GAS TURBINE COMPRESSOR SURGE MARGIN

Dr. Vivek Sahai
Cheng Fluid Systems, Inc.
480 San Antonio Road, Suite 120
Mountain View, CA 94040

Dr. Dah-Yu Cheng
Cheng Fluid Systems, Inc.
480 San Antonio Road, Suite 120
Mountain View, CA 94040

ABSTRACT

In many industrial gas turbine compressor designs, the compressors later stage blade angles are reduced in a constant flow area section as a means to even out the per stage workload. Most compressors use NACA 65 series type airfoils, which are good for high subsonic and supersonic flow, but are poor for middle or low subsonic flows. The temperature increases as the compression ratio increases; which cause the Mach number to drop. With reduced blade cascade overlaps, a reduction in axial blade solidity results. The compounding effect of low solidity and a low Mach number can cut the stalling angle by several degrees. This recent study found that compressor stall more or less is linked to the change of moment coefficient Cm, rather than lift coefficient Cl. Designing the airfoil, by extending the constant moment coefficient to a higher angle of attack region can delay the trailing edge upper surface separation to a higher angle of attack, the main source of rotating stall. This separated flow exhibits itself more clearly on the moment coefficient, but is obscured by an increase in lift coefficient before "aerodynamic" stall. This new design is based on the second order derivative of the camber line, with a low drag symmetrical airfoil thickness. Numerical simulation of a single airfoil and cascade of the new airfoil is compared with other shapes. The results show that the trailing edge flow separation begins at a 9.5-degree angle of attack for the NACA 65 series airfoils. The NACA 0012 separation (i.e. change in Cm) starts at 5 degrees (total stall occurs at 11 degrees). The new airfoil CFS18-0010 exhibits no separation for a single airfoil of up to 12 degrees. The cascade results showed no flow separation up to an angle of 15 degrees, which is enough to eliminate most of the rotating stall.

INTRODUCTION

Compressor surge is the limiting factor for a number of aircraft and gas turbine operators. This paper addresses the surge margin issue in the later stages of the axial flow compressor. In aircraft gas turbines, high angles of attack at the inlet can cause flow distortions (a source of compressor stall) as the plane goes through maneuvers. These distortions create high stresses on the blades, stalls, and flameouts in the gas turbine. Ground based turbines and certain industrial turbines can reach stall conditions during cold weather, which can limit the turbines output potential. When low BTU fuels are used, they require higher mass flows through the turbine, and that creates a higher backpressure on the compressor. Very little can be done about inlet distortion in an aircraft turbine. If the later stages of a compressor are powerful enough to provide suction, the front stage distortion will not cause the compressor in general to stall.

For certain industrial gas turbine compressor designs, the compressor blade section angles are reduced (instead of reducing the cross sectional area) to distribute the per stage workload. Most gas turbine compressors use NACA 65 series type airfoils, which are good for high subsonic and supersonic flow, but are aerodynamically inefficient when the Mach number drops to values for low and middle subsonic flow (such as 0.5 and 0.6)(Johnson and Bullock, 1965). When temperatures in the later stages of the axial compressor increase, they are subjected to lower Mach number flows. With the high rotation of the blade stagger angles in the later stages of the axial compressor; this causes a reduction in the axial solidity. The compounding effect of low solidity and a low Mach number can cut the stalling angle by several degrees.

In this paper we focused on the phenomenon of moment coefficient Cm rather than lift coefficient Cl, as the indication of when flow separation off the upper surface at the trailing edge occurs, which can cause compressor stall. In a majority of airfoils, Cm is a constant from 0 to a low angle of attack then rapid changes occur. The authors attribute this to the upper trailing edge surfaces flow separation. When the upper surface trailing edge flow separation begins, the Cm increases due to a loss of lift at the trailing edges upper surface. This report describes a new airfoil design that starts with a minimum second order derivative for the leading edge and trailing edge, which we found is related to the pressure differential between the upper and lower surfaces of the airfoil. Separation at the leading edge can lead to localized shock waves. Separation on the trailing edge can lead to an upper surface flow separation. Both types of separation have a profound effect on compressor efficiency and stall characteristics. First, data showing the effect of axial solidity, stagger angle, and Cm behavior for other airfoils are discussed. Numerical simulation of a single airfoil and a cascade with the new airfoil design is compared with other shapes. The results show no upper surface separated flow for a CFS series airfoil design with a comparable turning angle and thickness; as a NACA 65 series thickness compressor blade of up to an angle of attack of 12 degrees; and the cascade results showed no separation up to an angle of attack of 15 degrees, which should be enough to eliminate most of the problems with stall.

NOMENCLATURE

Cd	Drag coefficient
Cl	Lift coefficient
Cm	Moment coefficient
C	Blade chord length
Cx	Axial chord
Ds	Suction surface diffusion parameter
Ma_2	Mach number at exit of blade cascade
S	Blade spacing
U	Rotor speed
α	Angle of attack
β	Stagger Angle
γ	Specific heat ratio
σ_x	Axial Solidity (Axial Chord/ Spacing)

BACKGROUND

An axial flow compressor consists of various sections that contain inlet and exit guide vanes, and rotor and stator blade cascades. The stator blade sections convert the kinetic energy from the rotor section to pressure. The performance of the compressor is determined by the blade performance. Stall in the compressor is the result of a flow disturbance on the upper surface of the blade as illustrated in Figure 1(Harmon, 1981). This is the seed to initiation of the classical rotating stall phenomenon (Day, Greitzer, and Cumpsty, 1978; Grietzer, 1981).

The key to understanding the performance of a compressor blade cascade are the parameters of axial solidity and stagger angle as illustrated in Figure 2 (Stewart, and Glassman, 1994; Johnson and Bullock, 1965). The axial solidity is defined as the ratio of axial chord over blade spacing (σ_x = Cx / S). The blade spacing is measured from the tip to tip between blades. The axial chord as shown in Figure 2 depends on the stagger angle of the blade (Cx = C*cosine β). For blade cascade axial solidities of 1 or greater channel flow exists. If the blade spacing is high or the blade stagger angle is high, the blade cascade axial solidity decreases. The effect of high stagger angle and low axial solidity is illustrated for NACA 65 series type blades with a 10% maximum thickness in Figure 3 (Emery, et al, 1958). Most compressors use this type of blade in their designs. Figure 3a shows the lift and drag behavior for a cascade of blades with a stagger angle of 30 degrees and axial solidity of 0.87. The data show that the angle of attack at which stall occurs is 21 degrees. This angle of attack is 75% higher than that for a single blade (Abbot and Von Doenhoff, 1959). Figure 3b shows the effect of lift and drag behavior for a blade cascade with a blade stagger angle of 60 degrees with the axial spacing the same as in Figure 3a. The higher blade stagger angle lowers the axial solidity to 0.5. The lower axial solidity causes the stall angle to occur sooner at an angle of attack of 15 degrees. The stalling angle is cut by at least one-fourth.

For decreased blade axial solidity the interaction between the blades is lessened and the single blade performance characteristics become important. The aerodynamic definition of stalling is based on the lift and drag coefficients' behavior. However, before stall occurs for most airfoils, changes in the moment coefficient behavior can represent separated flow off the upper surface of the airfoil before total stall. Figure 4 (Carpenter, 1958; Gregory and Wilby, 1973) plots the lift and moment coefficient behavior for a NACA 0012 airfoil for Mach numbers ranging from 0.3 to 0.75. As the Mach number increases, the angle of attack before aerodynamic stall occurs decreases. For example at a Mach number of 0.6, the maximum lift coefficient is 0.95 and aerodynamic stall occurs at an angle of attack of 11 degrees. However the moment coefficient starts to change at an angle of attack of 5 degrees. Simulations were performed to predict the turbulent compressible flow behavior around this airfoil at an angle of attack of 8 degrees at an inlet Mach number of 0.6. The industry standard k-ε turbulence model was used for all the STAR-CD (1999) two-dimensional simulation work. Figure 5 shows the results from this simulation. The Mach number variation around the airfoil (Figure 5a) shows that there is an increase of the Mach number to slightly above 1 on the top surface and a low Mach number region on the trailing edge of the upper surface of the airfoil. This is a region of separated flow as illustrated by the streamlines in Figure 5b. This trailing edge separation can cause problems in blade cascades if the axial solidity is low.

A velocity vector analysis can provide information on how the flow changes in the axial direction from stage to stage. Slower axial velocities can lead to a more positive angle of attack on the blades (Johnson and Bullock, 1965). Stewart and Glassman (1994) have shown that the required axial solidity for a blade cascade depends primarily on the Mach number at the exit of the blade cascade (Ma_2). In equation form this can be expressed as (Stewart and Glassman, 1994):

$$\sigma_x = 1 - [(Ma_2)^2 / (\gamma+1)] + [(D_s * (Ma_2)^2) / (2\gamma + 2)] \quad (1)$$

In equation 1, γ is the specific heat ratio (1.4 for air) and D_s is known as the suction diffusion parameter which is a measure of the flow deceleration on the blade suction surface. Most blade cascades are designed so that this parameter varies between 1 and 2 (Stewart and Glassman, 1994). Figure 6 (Stewart and Glassman, 1994) shows the required axial solidity for several values of exit Mach number. When the exit Mach number is 1 and above, the required axial solidity is low (around .7 to 0.8 for a D_s of 1). However when the exit Mach number drops to below 1, the required axial solidity increases (for example an exit Mach number of 0.6 needs an axial solidity of 0.925). Thus, low exit Mach numbers require high values of axial solidities for good blade cascade performance (Stewart and Glassman, 1994).

Certain designs of axial compressors for gas turbines have constant annular area sections for the later stages. In this region, the blade angles are reduced to distribute the per stage workload. Most compressors use NACA 65 series airfoils. These airfoils are aerodynamically inefficient for low subsonic Mach number flows (Johnson and Bullock, 1965). Typical compressor blades are twisted and have varying thickness and shapes from the tip to the base. This affects the blade cascade characteristics. Figure 7a shows the measurements of the stagger angle for the hub and tip from an actual industrial gas turbine compressor for the later stages where the annulus area is constant. Note that the blade stagger angles for the hub are relatively low. The tip blade stagger angles are high and starting at the 13^{th} stage they go above 55 degrees. These high blade stagger angles result in solidities dropping around 0.5 after the 13^{th} stage at the tip as shown in Figure 7b. The maximum thickness at the tip was 6% and hub was 13.5%. The mid section of the blade had a thickness of approximately 10%. Information from Abbot and Von Doenhoff (1959) shows the lift coefficient and moment coefficient behavior for the single blade. The moment coefficient as shown in Figure 8 starts to drop at 9.5 degrees before the blade stalls at 10 degrees.

For these later stages, the increased compressor ratio causes the temperature to increase. This causes the Mach number to drop. The high blade stagger angle reduces the blade cascade overlaps. The compounding factors of low axial solidity and a low Mach number can cause trailing edge separation to start sooner and stalling can occur. Also, as the ambient temperature drops, the inlet angle of attack to the blade cascade can increase due to the reduced axial velocity (Johnson and Bullock, 1965). This trailing edge separation is illustrated in Figure 9, which shows the Mach number variations over the 16^{th} stage compressor blade tip cascade at angles of attack of 11 degrees and 15 degrees. The blades maximum thickness is 6% and the camber line of the blade is shown in Figure 10c. The NACA 65 series blade thickness was applied to this camber line. Due to the high stagger angle of 61 degrees at this stage, the axial solidity is at 0.45. The inlet Mach number to the blade cascade is 0.6. The results show that there is upper surface trailing edge separation. The high blade stagger angle reduces the blade-to-blade interaction.

NEW AIRFOIL DESIGN

To improve the aerodynamic behavior in the later stages of the compressor, a new airfoil design has been created. This airfoil design addresses the moment coefficient behavior. Addressing the moment coefficient properly, a single airfoil can extend the constant Cm behavior to a higher angle of attack without trailing edge upper surface separation, the main source of rotating stall. This design is based on the second order derivative characteristics of the camber line as shown in Figure 10a. The boundary conditions for this derivative are that the values at the leading edge and trailing edge are approximately zero. A comparison with the currently used compressor blade is also shown in Figure 10a. It can be seen that the second derivative has the highest positive values at the leading edge and trailing edge. In contrast, the new design has the highest values of the derivative are in the middle. It is our belief that this changes the characteristic of the flow. The second order derivative is related directly to pressure distribution. The non-zero second order derivative at the trailing edge for the compressor blade leads to early upper edge separation.

The next step in the analysis was to integrate twice the second order derivative behavior to obtain the first derivative and the physical camber line of the new airfoil. This integration was performed and is shown in Figures 10b and 10c. Figure 10b shows the first derivative after integration for the new foil and compares it with the current NACA 65 series blade. The integration constant was set so that the turning angle of the blade is preserved.

The shape of the camber line for the new design as shown in Figure 10c has been used in a rotation vane design (Golomb, Sahai, and Cheng, 2002; Sahai and Golomb, 2000; Kosla and Mutsakis, 1992) that removes the turbulence caused by fluid moving through an elbow or curved conduit. This new design was used to remove the Kutta condition (McCormick, 1995) at the trailing edge. The uniqueness of the vane technology is that it is flow rate independent (Kosla and Mutsakis, 1992). The vanes used in this device are contoured using this approach.

After the camber line was obtained, a low drag symmetrical airfoil thickness was applied. Two airfoil geometries were studied: CFS18-0010 and CFS18-0006. The numbering scheme for this airfoil is that the first two numbers represent the turning angle (in this case 18 degrees). This is the same turning angle for the current NACA 65 series compressor blade. The last four numbers represent the same number scheme for the NACA 4 digit airfoils (Abbot and Von Doenhoff, 1959). The two maximum blade thicknesses studied correspond to the tip and mid plane thickness of the original compressor blade discussed in the previous section.

NEW AIRFOIL DESIGN RESULTS

Simulations were performed with the new airfoil design to determine the flow behavior for various angles of attack. Single blade simulation results for the CFS18-0010 airfoil showed that the moment change did not occur until an angle of 12 degrees. Figure 11 shows the CFS18-0006 blade cascade results for angle of attack of 11 degrees and 15 degrees. The inlet Mach number was 0.6 for both cases. The stagger angle was 61 degrees and axial solidity was 0.45, similar to the compressor blade results shown in Figure 9. No upper surface trailing edge separation was noticed on the middle blade of the cascade for both cases. Figure 12 shows a similar result at an angle of attack of 15 degrees for the blade cascade for the CFS18-0010 blade. The new blade cascade delays the upper surface trailing edge separation to an angle of attack of 15 degrees, which should be enough to eliminate most of the rotating stall problems. This upper surface separation contributes to loss in compressor efficiency. This new design can improve compressor efficiency and performance by minimizing the upper surface separation.

CONCLUSIONS

The moment coefficient is usually constant to a certain range of angle of attack and then dramatically changes due to upper surface trailing edge separation. This does not sensitively affect the lift coefficient but it affects the drag coefficient so ordinarily aircraft designers do not pay much attention to the moment coefficient. For gas turbine designers, the upper surface separation could be a source triggering the devastating rotating stalls and extending the angle of attack before separation begins by just a few degrees, which can dramatically extend the surge margin and efficiency of a compressor. The new airfoil design without a symmetrical airfoil thickness (called a Cheng Rotation Vane) has been used in straightening pipe flow. This design eliminated the velocity dependence on the exit angle on the trailing edge, and has been used for 12 years in the refinery industry. This new airfoil design extends that prior experience. The methodology of using the second derivative to prescribe the pressure distribution, then integrating twice to get the actual camber line geometry, and applying a low drag thickness, seems to accomplish the extension of the angle of attack for the later stage compressor blades. This paper has addressed this problem with numerical simulations. It is our intent to follow up this theoretical work with experimental results to determine the effectiveness of the new blade design on compressor performance.

ACKNOWLEDGMENTS

The authors would like to thank Audie Mak for his assistance in making the compressor rotor blade cascade measurements and his assistance in implementing the new blade design philosophy. The authors would also like to thank Richard Golomb and Ian Church for their assistance with this paper.

REFERENCES

Harmon, R.T.C., 1981, Gas Turbine Engineering Applications, Cycles, and Characteristics, John Wiley & Sons, Inc. NY, NY, pg. 133-134

Day, I.J., Greitzer, E.M., and Cumpsty, N.A., 1978, "Prediction of compressor performance in rotating stall," Journal Engineering Power, Volume 100, pp. 1-14

Greitzer, E.M., 1981, "The Stability of Pumping Systems – The 1980 Freeman Scholar Lecture," Journal of Fluids Engineering, Volume 103, pp. 193-242.

Stewart, W.L., and Glassman, 1994, A.J., Turbine Design and Application, NASA SP-290

Emery, J.C., Herrig, L.J., Erwin, J.R., Felix, A.R., 1958, "Systematic Two-Dimensional Cascade Tests of NACA 65-Series Compressor Blades at Low Speeds", NACA Technical Report 1386

Carpenter, P.J., 1958, "Lift and Profile Drag Characteristics of an NACA 0012 Airfoil Section As Derived From Measured Helicopter-Rotor Hovering Performance", NACA Technical Note 4357

Gregory N., and Wilby, P.G., 1973, "NPL 9615 and NACA 0012: A Comparison of Aerodynamic Data", ARC C.P. Number 1261

STAR-CD (1999) Version 3.10 Methodology, Computational Dynamics Ltd.

Johnson, I.A., and Bullock, R.O., 1965, Aerodynamic Design of Axial-Flow Compressors, NASA SP-36

Abbot, I.H., and Von Doenhoff, A.E., 1959, Theory of Wing Sections Including a Summary of Airfoil Data, Dover Publications, NY, NY

Sahai, V., and Golomb, R., 2000, "Improve Condenser Water Flow to Improve Cash Flow," Volume 144, No. 4, Power Magazine, July/August pp. 62-64

Kosla, L., and Mutsakis, M., 1992, "New In-Pipe Flow Conditioner Cuts Fluid Turbulence Problems", Chemical Engineering Magazine, September

Golomb, R., Sahai, V., and Cheng, D.Y., 2002, "A New Tailpipe Design for GE Frame Type Gas Turbines to Substantially Lower Pressure Losses", ASME Turbo Expo 2002, Amsterdam, The Netherlands, June, GT-2002-30149

McCormick, B.W., 1995, Aerodynamics, Aeronautics and Flight Mechanics, Second Edition, John Wiley & Sons, Inc., NY, NY

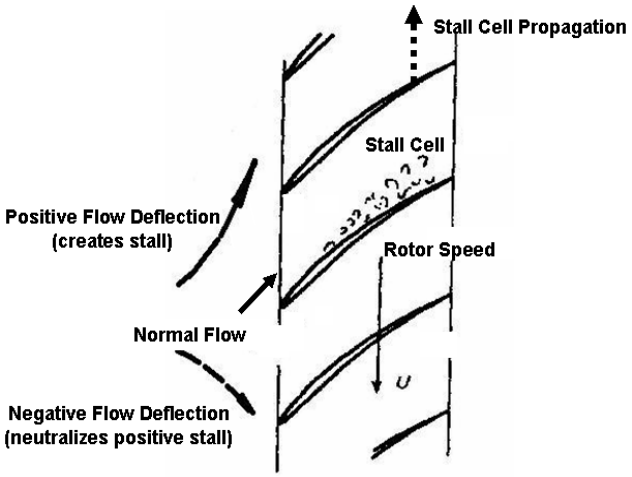

Figure 1. Upper Surface Trailing Edge Separation can lead to the initiation of Rotating Stall

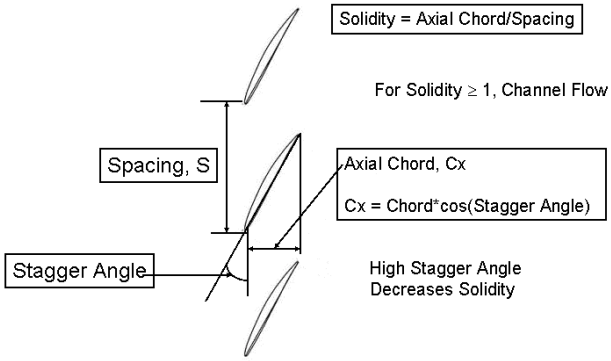

Figure 2. Definition of Axial Solidity and Stagger Angle for a Blade Cascade

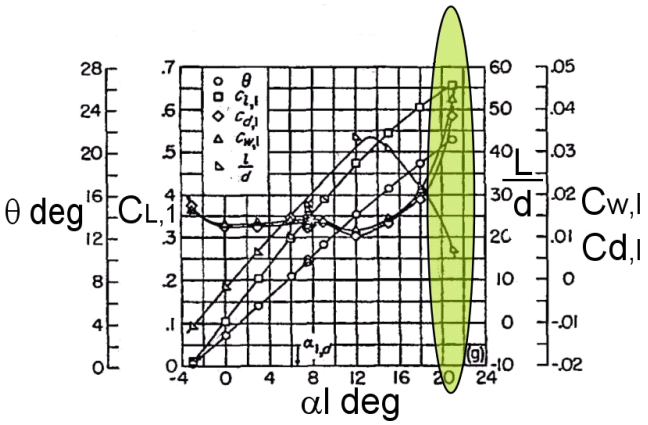

a

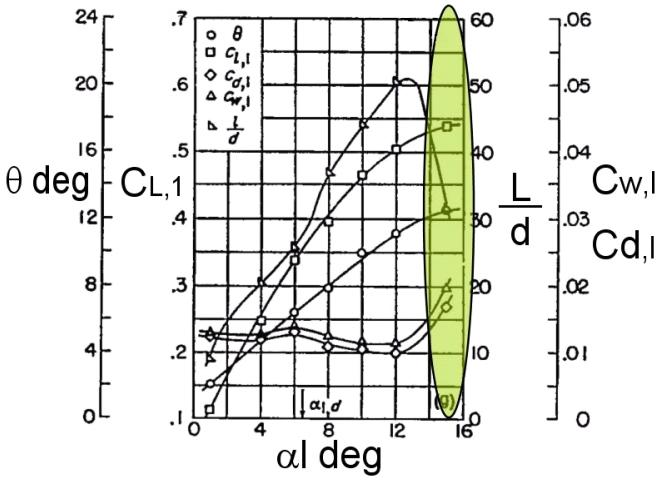

b

Figure 3. If the Stagger Angle is High and the Axial Solidity Low, then the Stalling Angle can be reduced by several degrees for NACA 65 Series Blades. a) Results for a stagger angle of 30 degrees and axial solidity of 0.87 show stalling angle of 21 degrees (as marked). b) For same blade spacing and blade stagger angle of 60 degrees, the axial solidity decreases to 0.5. The results show the angle of attack at which stall occurs is now 15 degrees.

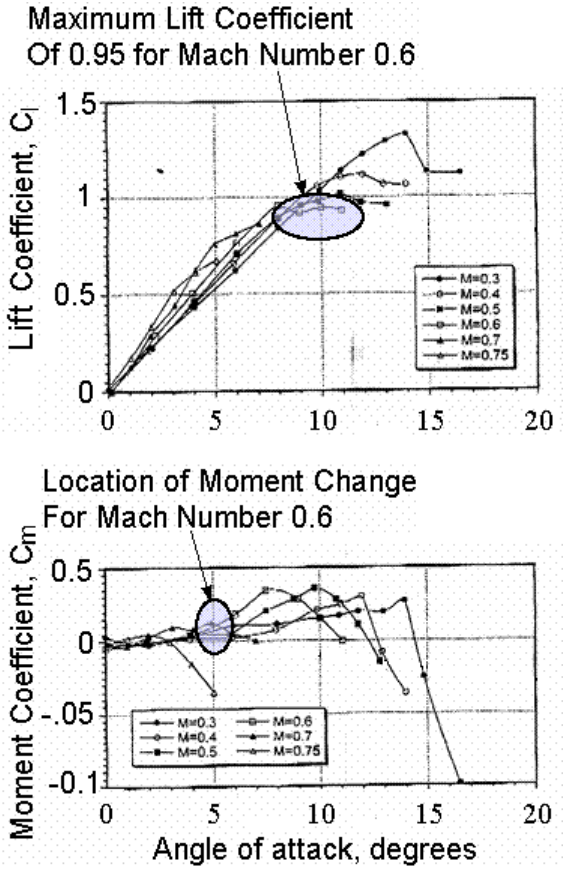

Figure 4. Lift and Moment Coefficient Behavior for NACA 0012 Airfoil for Mach numbers from 0.3 to 0.75

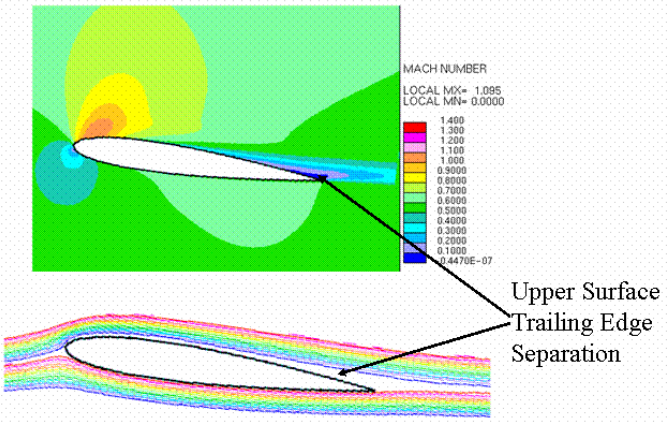

Figure 5. Mach Number Variation and Streamline paths over a NACA 0012 Airfoil at an Angle of Attack of 8 Degrees and Inlet Mach Number of 0.6

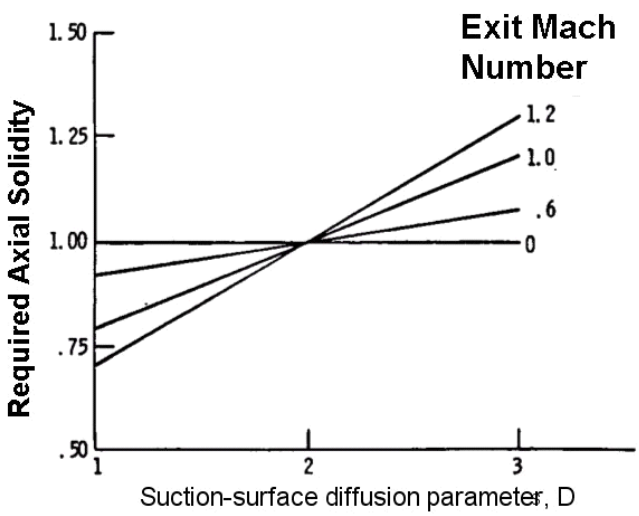

Figure 6. Required Axial Solidity depends on Exit Mach Number and Suction Diffusion Parameter

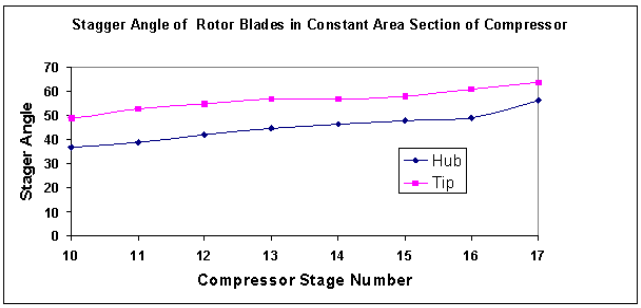

Figure 7a. Stagger Angle Measurements for the tip and hub from a Typical Axial Compressor in the Constant Area Section. The stagger angle goes above 55 degrees starting at the 13th stage.

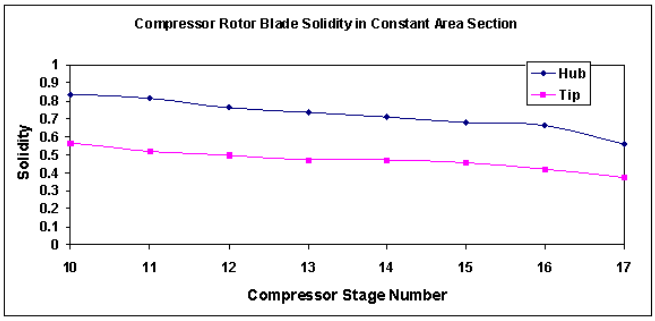

Figure 7b. Axial Solidity for this same compressor shows the hub axial solidity stays high while the tip drops to around 0.5 starting at the 13th stage.

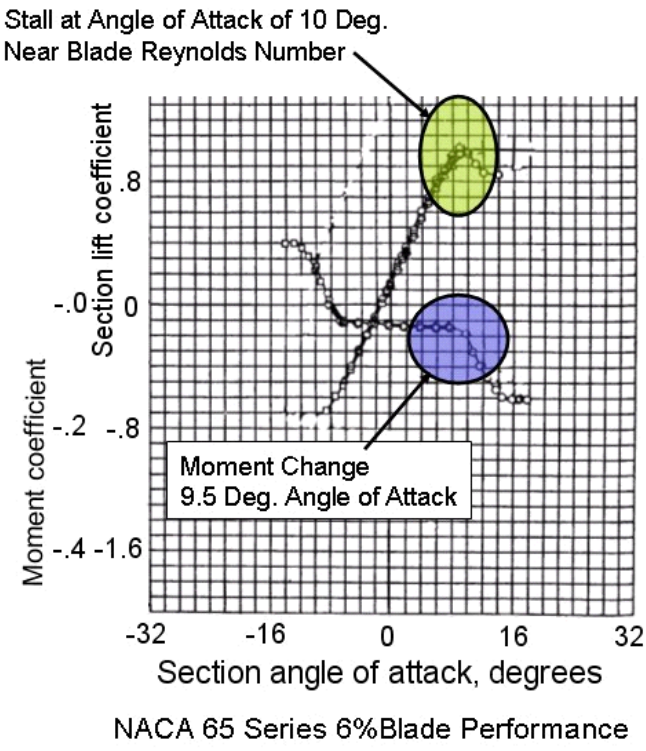

Figure 8. Blade Performance Data for NACA 65 Series 6% Blade showing Moment Change at 9.5 Degrees Angle of Attack

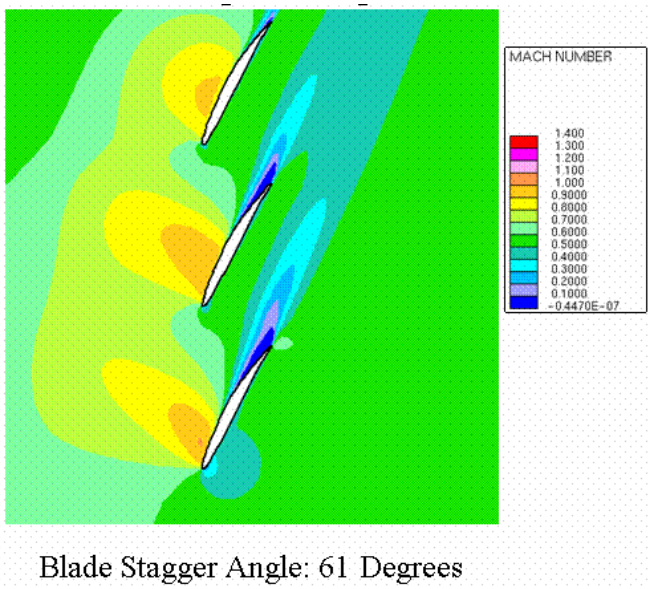

a

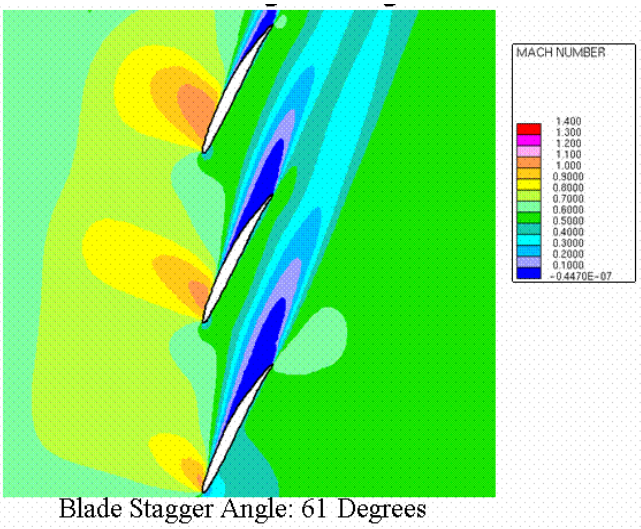

b

Figure 9. a) 16th Stage Current Compressor Blade Design Cascade Mach number Variation at 11 Degrees Angle of Attack
b) 15 Degrees Angle of Attack
The inlet Mach number is 0.6 and axial solidity is 0.45. Due to the low axial solidity, both sets of results show significant trailing edge upper surface separation.

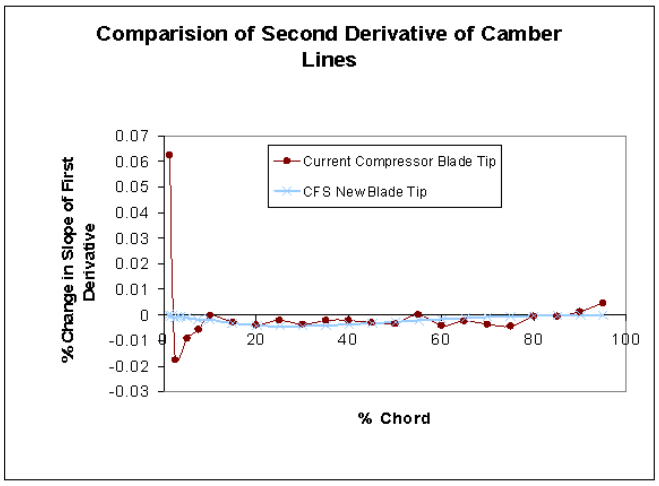

a

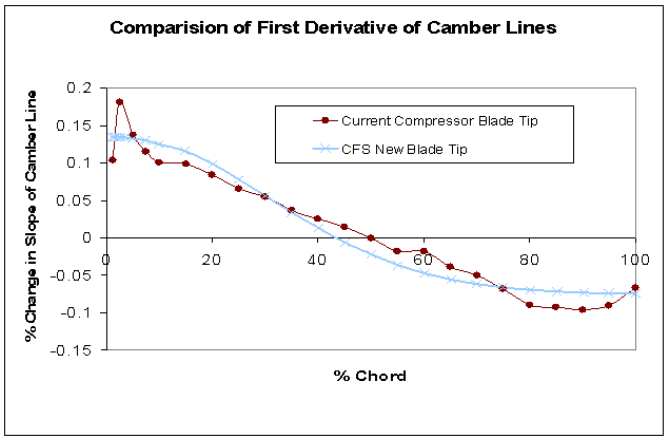

b

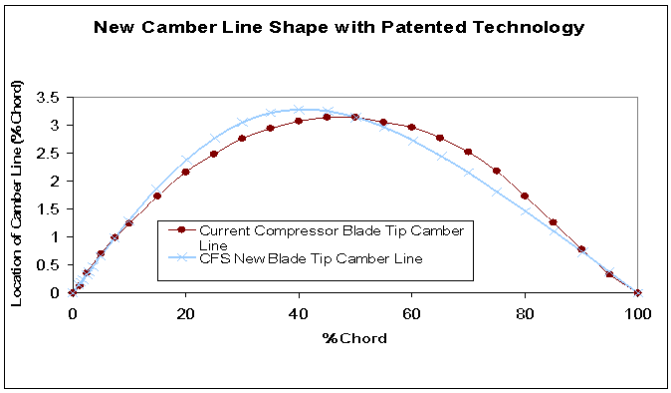

c

Figure 10. New Airfoil Design vs. Current Compressor Blade Comparison of Second, First and Physical Camber Line a) Second Derivative of New Design is 0 at leading and trailing edges b) First Derivative and c) Camber Line

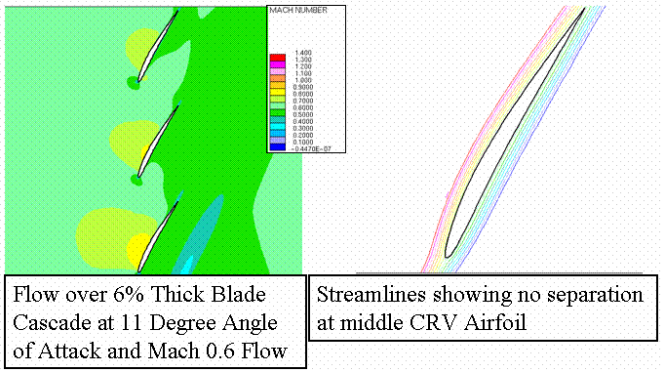

a

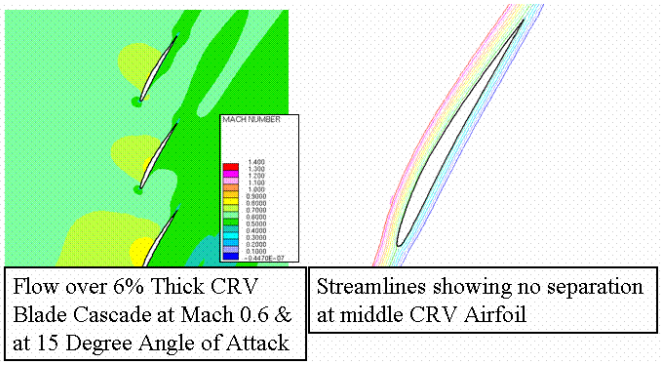

b

Figure 11. New Airfoil Design CSF18-0006 Blade Tip Cascade a) 11 Degrees Angle of Attack and b) 15 Degrees Angle of Attack. The inlet Mach number is 0.6 and the axial solidity is 0.45. Note that the upper surface trailing edge separation is removed

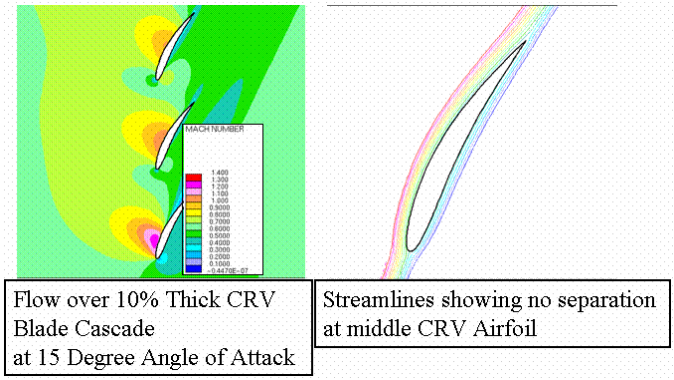

Figure 12. New Airfoil Design CSF18-0010 at 15 Degrees Angle of Attack for an inlet Mach number of 0.6 and axial solidity of 0.45. Note that the middle blade does not show any upper surface trailing edge separation.